energies

MDPI

Article

Characterization of Thermophysical Properties of Phase Change Materials Using Unconventional Experimental Technologies

Arnold Martínez [1,2], Mauricio Carmona [1,*], Cristóbal Cortés [3] and Inmaculada Arauzo [3]

1 Rational Use of Energy and Environment Preservation Research Group from Universidad del Norte, 081007 Barranquilla, Atlántico, Colombia; arnoldg@uninorte.edu.co

2 Engineering, Science and Technology—I.C.T Research group from Universidad de Córdoba, 230002 Montería, Córdoba, Colombia

3 Department of Mechanical Engineering, University of Zaragoza, Campus Río Ebro. Building B. María de Luna s/n, 50018 Zaragoza, Spain; tdyfqdb@unizar.es (C.C.); iarauzo@unizar.es (I.A.)

* Correspondence: mycarmona@uninorte.edu.co

Received: 31 July 2020; Accepted: 3 September 2020; Published: 9 September 2020

Abstract: The growing interest in developing applications for the storage of thermal energy (TES) is highly linked to the knowledge of the properties of the materials that will be used for that purpose. Likewise, the validity of representing processes through numerical simulations will depend on the accuracy of the thermal properties of the materials. The most relevant properties in the characterization of phase change materials (PCM) are the phase change enthalpy, thermal conductivity, heat capacity and density. Differential scanning calorimetry (DSC) is the most widely used technique for determining thermophysical properties. However, several unconventional methods have been proposed in the literature, mainly due to overcome the limitations of DSC, namely, the small sample required which is unsuitable for studying inhomogeneous materials. This paper presents the characterization of two commercial paraffins commonly used in TES applications, using methods such as T-history and T-melting, which were selected due to their simplicity, high reproducibility, and low cost of implementation. In order to evaluate the reliability of the methods, values calculated with the proposed alternative methods are compared with the results obtained by DSC measurements and with the manufacturer's technical datasheet. Results obtained show that these non-conventional techniques can be used for the accurate estimation of selected thermal properties. A detailed discussion of the advantage and disadvantage of each method is given.

Keywords: thermal energy storage; phase change materials; thermophysical characterization; T-history; T-melting CHF

1. Introduction

The interest in phase change materials (PCM) grows continuously due to its wide application in sectors as the storage of solar thermal energy, industrial heat recovery, construction, agricultural greenhouses, aerospace, health, refrigeration, among others [1–3]. An adequate characterization is a mandatory requirement for numerical modeling of processes involving PCM, equipment design, and the development of this technology and its applications, since thermal characterization provides information about the amount of energy that a material can store. There are multiple thermal properties that must be defined for an adequate characterization of the PCM. Most of the existing standards were not developed specifically for thermal storage applications. However, they are currently used as the basis for determining the thermal properties of these kind of materials [4].

Among the main standards applied to the characterization of PCMs using DSC, the following technical standards are distinguished: ASTM D87, which is the standard test method for melting point of petroleum waxes; ASTM D4419 for measurement of transition temperatures of petroleum waxes; ASTM E793, which is a standard method to determine enthalpies of fusion and crystallization with DSC. Similarly, there are more standards that are used for the determination of thermal conductivity, which depend on the measurement devices, as well as other standards for determination of density, viscosity, among others. These standards are applicable since there is currently no exclusive standard for PCMs, and they are applied more as a general use of the measuring device.

In the last thirteen years, several authors have worked in the development of standards for PCM, being notable the contributions especially in the determination of thermophysical properties by DSC. Differential scanning calorimetry is the most robust technique for determining the phase change enthalpy, there are several criteria that must be considered when characterizing a PCM with this technique [5], for example, (i) the type of calorimetry, which can be made in dynamic or step mode. In this sense, Barreneche et al. [6] did not observe significant differences between both methods for paraffins. (ii) the heating/cooling rate. As is proposed by Mehling et al. [7], a thermal equilibrium must be achieved, which only can occurs at low heating/cooling rates, since high ramps of velocity generate artificial effects such as hysteresis and (iii) the mass of the sample must be constant. Günther et al. [8] found that the signal peak shifts towards higher temperatures as the mass or heating rate increases.

Other procedures have been developed in recent years to standardize DSC measurements such as equipment calibration, determination of the required cooling/heating rate, experimental procedure, and representation of the obtained data [9]. Some of the recommendations for traceability in measurements suggest very extensive tests, which involve testing at different cooling/heating rates until, for example, in the case of the enthalpy-temperature curve in the DSC the maximum value in temperature differences cannot exceed the limit of 0.2 K. The quality criteria and measurement methods for PCM were established by the ZAE Bayern research center and the Fraunhofer ISE, and since 2008 the RAL label has been awarded to products that have been tested under these exhaustive monitoring and testing time criteria [10].

Specific heat is also other important property in the characterization of PCM, especially the values before and after the phase change (solid and liquid phase). In this case, the ASTM E1269 standard is used for the determination of the specific heat by differential scanning calorimetry, however Ferrer et al. [11] compared the dynamic, isostep and area methods, finding that the results obtained by the area method had an error lower than 3%, while the dynamic and the isostep errors up to 6% and 16%, respectively. Thermal conductivity can be measured by different methods, but the three main measurement methods used are: (i) hot disk, (ii) hot wire and (iii) laser flash, each of these techniques require specialized equipment and are mainly based on ISO 22007, ASTM D7896, ASTM E1461.

Other devices for measuring thermal properties are especially required when evaluating large or non-homogeneous samples, as material encapsulated in polymeric matrices or expanded graphite, likewise composite materials for the construction industry, textile, among others. Cabeza et al. [12] presented a series of devices that were built for the determination of properties, among which stand out for the measurement of enthalpy-temperature, diffusivity, and thermal conductivity curves.

The T-history method was proposed by Yinping & Yi [13], this requires three measurements during the cooling process of a PCM sample with unknown properties and a reference substance with well-known thermal properties, which are cooled in ambient air, that is monitored too. The cooling curve of the sample and the reference are recorded, from an initial temperature value, higher than the melting temperature of the sample until both reach an ambient temperature. Some improvements have been proposed to the original method over the years, in which the values of specific heat (cp) and enthalpy (h) can be calculated as temperature dependent values using the same experimental procedure [14]. Reference [15] applied the T-history method to a wide variety of PCMs such as paraffins and lauric acid having no or low degree of supercooling. While some authors propose assemblies with the test tubes arranged in a vertical position according to the original method [15], others propose the

horizontal configuration to avoid the temperature difference in the tube [16]. With T-history also is possible estimate of the "effective thermal capacity" cp_{eff} (T), which contains more information than any other phase change property [17].

Comparative results between measurements of dynamic DSC, step mode DSC and T-history, show that the precision of the latter is similar, but allows the investigation of large samples, which is crucial for heterogeneous materials like composite PCM or salt hydrates [8]. There are many investigations that have been carried out taking as reference the T-history for the determination of the thermophysical properties [18], some salt hydrates like disodium hydrogen phosphate dodecahydrate, sodium acetate trihydrate and STL-47 have been evaluated by this method [19]. The thermophysical properties of other PCMs such as paraffin waxes, salt hydrates and mixtures of fatty acids have also been evaluated by T-history and compared by DSC results [20]. Thermophysical properties for alcohol, WFI, Greek paraffin, RT20, RT27, RT58, SP25A8 are reported in the literature [21]. Other non-homogeneous materials have been evaluated by t-history method, this is the case of the commercial sodium acetate trihydrate-based PCM (Climsel C58), which was blending with additives for their characterization [22]. Five paraffin waxes and wood resin (all available in Indian market) were investigated to determine their suitability as a thermal energy reservoir in solar drying applications [23]. Also, this method has been adapted to be able to determine the latent heat in some granular phase change composites like RUBITHERM GR27 and GR41 EPCM [24]. PCM for air conditioning applications, such as semiclathrate hydrates of tetra-n-butylammonium fluoride (TBAF) have been evaluated by this method, confirming that the T-history method is a practical method to determine the phase change enthalpy of hydrates [25]. Recently, the use of T-history has been reported in nano-enhanced (NEPCM) applications, in which the thermophysical parameters of multiwall carbon nanotubes (MWCNT) in capric acid were obtained [26].

Some setups of the T-history have been made using insulated sample holders. In some cases the effects of the thermal mass of the insulation can be neglected using sample holders with a high ratio between the thermal mass of the PCM to the insulated sample holder [27], The evaluation method for insulated T-History measurements was reported taking into account the heat capacity of the insulation material [28]. The T-history has critically assessed based on their mathematical formulation and experimental configuration [29]. The effect of radial thermal gradients inside T-history samples on the enthalpy temperature curve measurement have been analysed [30], and has been and has been proposed a differential formulation of the T-History method in order to achieve thermodynamic consistency with phase transitions theory, including the experimental effect of the speed of the thermal process in calorimetric calculations [31].

In the present work, the T-history method was used to determine the enthalpy-temperature curves, on which the specific heat in solid and liquid phase are also obtained, this method was used due to its simplicity and low cost, results were comparing with measurements in DSC. However, both methods have their limitations, which generate convenience in the use depending of the application case, for instance, in the case of samples with subcooling phenomenon, the use of T-history is recommended, since with the DSC is not possible to obtain a representative measure of the enthalpy variation with temperature [32]. If the sample of material to be tested is not pure and/or non-homogeneous, it is more useful the use T-history, since the sample sizes used in DSC is only a few milligrams, while for the T-history reach several grams, it is a greater challenge to obtain a representative sample in non-homogeneous materials if the sample size is to small [12].

One of the major limitations of the original T-history lies in temperature control, which is performed at room temperature [13]. However, researchers at ZAE-Bayern [32] proposed configurations where tests between −20 to 65 °C could be performed, Kravvaritis et al. [17] added a cooling and heating system in which tests could be performed between −30 to 120 °C, Stankovic [33] used an environmental chamber with advanced temperature control, which operated in a temperature range between −10 up to 100 °C with an accuracy of ±0.2 °C. All these modifications contribute to the

reliability of the measurements, but they make the method much more expensive than the simplicity that characterized the original method.

The conventional method DSC have a small chamber in which samples are evaluated in much wider temperature ranges, typically between −90 °C up to 550 °C, depending on the heating and cooling system they have incorporated. Therefore, this is a versatile and robust equipment with the capability to evaluate almost all the organic and inorganic substances currently used in thermal storage applications.

Another proposed method for the determination of several thermophysical properties simultaneously was proposed in 2018 by Yang & Liu [34], in which Stefan's problem is solved in 1D with constant heat flow boundary condition, using a quasi-static fusion model, the method is known as "T-melting CHF".

This paper presents a general evaluation of two low-cost experimental methods (T-history and T-melting) proposed in the literature for the characterization of PCM, with a comparison of the results obtained by a specialized method (DSC) and the data provided by the manufacturer. Considering the simplicity and cost of the methods, these results can serve as the basis for determining properties in laboratories were specialized equipment for this purpose are not available. Likewise, the aim of this work is to establish a consensus between the difficulties and advantages presented by each method on the determination of the main thermophysical properties of PCM. In the first part, the experimental methods developed are presented, then the conditions and results of each of the tests developed are defined, and finally a comparison is made between the calculated properties and the effectiveness of each of the methods used.

2. Experimental Methods to Determine Thermal Properties

In any feasibility study or design process, estimation of the properties such as melting enthalpy, specific heat, thermal conductivity, and solid and liquid densities becomes important when performing the corresponding calculations. In this section, traditional measurement procedures for obtaining thermal properties is presented, and a comparison with low-cost alternatives is presented due to the need to know the main thermophysical characteristics of the materials to be used for particular applications that involve storage of thermal energy by latent heat.

2.1. Determination of Thermal Properties by DSC

Differential scanning calorimetry is the most common technique to determine phase transitions in inorganic compounds, polymers and foods. In this technique, the difference between the contributions of energy to a substance and a reference material is measured while both are subjected to a temperatures program at a controlled rate, while monitoring the difference in heat flux between them, as is shown in Figure 1 where the basic apparatus and the generated signals are described.

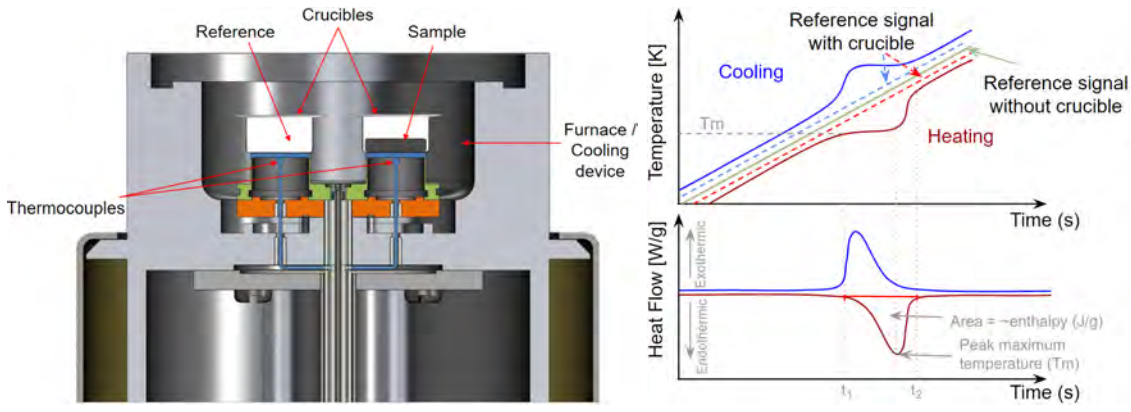

(**a**) (**b**)

Figure 1. (**a**) Schematic principle of DSC (**b**) Signal generation in a heat flux DSC.

Determination of heat capacity with a DSC can be made by three ways: directly, using a modulated DSC (MDSC) and the three run ASTM E1269 method. The latter requires baseline scanning, measurement to a standard sapphire sample and measurement to the sample material to be evaluated. Once the measurements are obtained, the specific heat of the sample $c_p(s)$ can be obtained by:

$$c_p(s) = c_p(st) \cdot \frac{D_s \cdot W_{st}}{D_{st} \cdot W_s} \quad (1)$$

where $c_p(st)$ is the specific heat capacity of the sapphire standard, D_s is the difference between the heat flow of the sample and the empty crucible at the same temperature, D_{st} is the difference between the heat flow of the sapphire and the empty crucible at the same temperature, W_s y W_{st} are the masses of the sample and the sapphire, respectively. According to Barreneche et al. [6], the calorimetries can be performed in dynamic mode or in step mode, without finding a significant difference between the two operation modes. In the case of salt hydrates, it is recommended the use of slow dynamic mode. ASTM D4419-90 standard for petroleum waxes recommends speeds of 20 and 10 K/min, however for organic and inorganic PCMs, the recommendation is the slow dynamic model with constant speeds of 0.5 K/min [6].

2.2. Determination of Thermal Properties Using the T-History Method

The T-history method basically consists of heating at least two test tubes, in which there is a sample material and a reference one, which are simultaneously heated in a thermostatic bath, at an higher temperature than melting point of the sample material. The interior temperature is recorded by thermocouples located in the center of the samples, which are connected to a data acquisition system. The scheme of the experimental setup used in this article is presented in Figure 2. Two test tubes are used for repeatabilty and water is used as the reference material. When the internal temperature stabilizes, the samples and the reference test tube are removed and are left to cool in a box of expanded polystyrene (EPS) under temperature-controlled environment. The cooling curves are plotted to monitor the test. The average time of each test is close to 4 h.

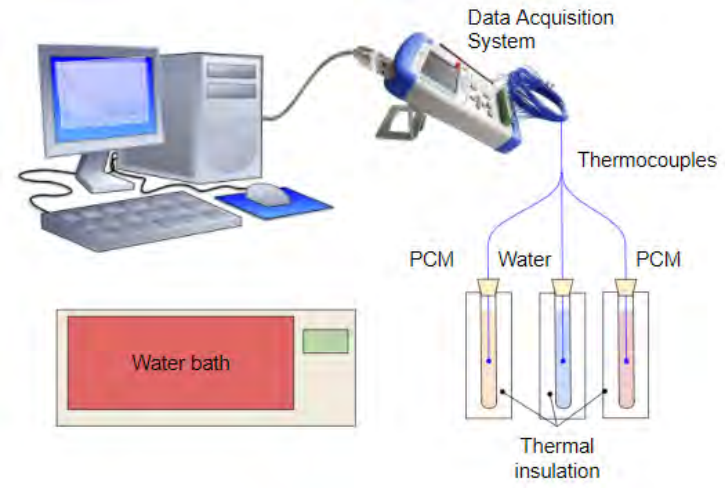

Figure 2. Scheme of the experimental setup for the implementation of the T-history method in cooling mode.

Some of the advantages of T-history are its relative simplicity and low cost, and since it is a non-commercial device, it is possible to carry out a particular assembly according to the specific range of the application to be evaluated. On the other hand, testing a sample of a representative size reduce the difficulty of crystallization associated with small samples, as occurs in the DSC. To be valid the hypothesis of lumped capacitance method (Bi < 0.1), the relationship between the length and the diameter of the tubes must be large enough (L/D > 10) [24].

Thermophysical properties are obtained with the equations derived from the original method and its subsequent improvements, the following expressions were used [14]:

$$c_{p,s} = \left(\frac{m_w c_{pw} + m_t c_{pt}}{m_p}\right) \frac{I_3}{I_2'} - \frac{m_t}{m_p} c_{pt}, \tag{2}$$

$$c_{p,l} = \left(\frac{m_w c_{pw} + m_t c_{pt}}{m_p}\right) \frac{I_1}{I_1'} - \frac{m_t}{m_p} c_{pt}, \tag{3}$$

$$H_m = \left(\frac{m_w c_{pw} + m_t c_{pt}}{m_p}\right) \frac{I_2}{I_1'} (T_0 - T_s), \tag{4}$$

where m is the mass, c_p is the specific heat, H_m is the phase change enthalpy, and the subscripts s and l refer to the solid and liquid phases, w, t and p they refer to water, tube and PCM, respectively. The values of I are presented in Figure 3, where the apostrophe represents the areas under the temperature-time cooling curve for distilled water.

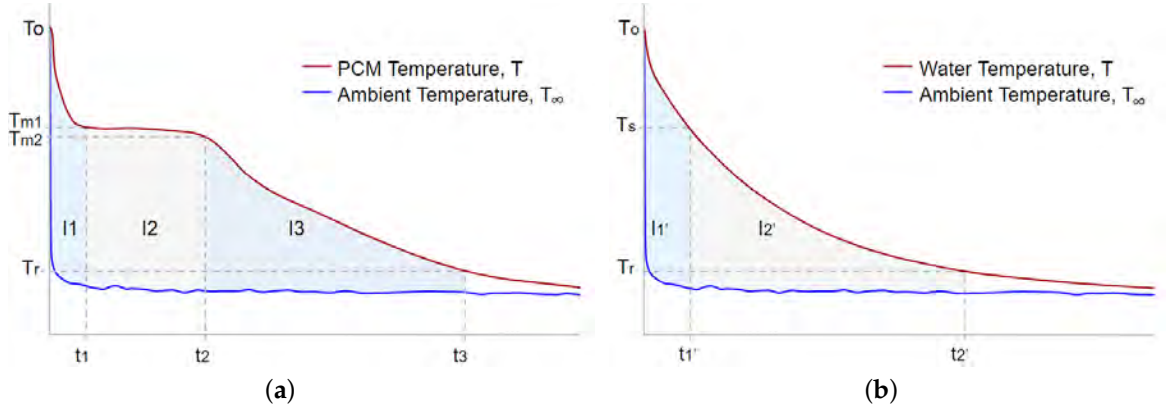

Figure 3. (**a**) Temperature–time curves for phase change materials (PCM) and ambient air; (**b**) Temperature–time curves for distilled water and ambient air [14].

Marín et al. [14] established that for impure materials that do not have a constant phase change temperature, in which the beginning of the phase change occurs in T_{m1} and the end in T_{m2}, the phase change enthalpy (H_m) can be calculated as:

$$H_m = \left(\frac{m_w c_{pw} + m_t c_{pt}}{m_p}\right) \frac{I_2}{I_1'} (T_0 - T_s) - \frac{m_t c_{pt} (T_{m1} - T_{m2})}{m_p}. \tag{5}$$

Additionally, they proposed the use of an motionless air chamber to obtain both heating and cooling curves, but their great contribution consists in allowing the calculation and subsequent plot of the enthalpy vs temperature, instead of using the concept of temperature variation with the time, where the change in the enthalpy of the PCM in the interval ΔT_i can be calculated as:

$$\Delta h_p(T_i) = \left(\frac{m_w c_{pw}(T_i) + m_t c_{pt}(T_i)}{m_p}\right) \frac{I_i}{I_i'} \Delta T_i - \frac{m_t}{m_p} c_{pt}(T_i) \Delta T_i. \tag{6}$$

The representation of the h-T curves can be obtained as the sum of the enthalpy intervals, assuming as a reference a given value of h_{p0}.

$$\Delta h_p(T_i) = \sum_{i=1}^{N} \Delta h_{pi} + h_{po}. \tag{7}$$

When the phase change of the PCM takes place in a temperature range, it is difficult to establish a limit between the phases. To identify these values, Hong et al. [15] used the first temperature derivative with the cooling curves to obtain a minimum peak value, which represents the end of the phase change.

Additionally, they included the average of the surface area of the tube containing the PCM and the reference (A_c and A'_c), Equations (2) and (3) to calculate $c_{p,l}$, $c_{p,s}$ are transformed into:

$$c_{p,l} = \left(\frac{m_w c_{pw} + m_t c_{pt}}{m_p}\right) \frac{A_c}{A'_c} \frac{I_1}{I'_1} - \frac{m_t}{m_p} c_{pt} \tag{8}$$

$$c_{p,s} = \left(\frac{m_w c_{pw} + m_t c_{pt}}{m_p}\right) \frac{A_c}{A'_c} \frac{I_3}{I'_2} - \frac{m_t}{m_p} c_{pt}. \tag{9}$$

Once the limits of the phase change are established for each of these regions, the heat of fusion is determined using the following expression [32]:

$$H_m = -\left(\frac{m_t}{m_p} c_{pt} + \frac{c_{p,l} + c_{p,s}}{2}\right) + \left(\frac{m_w c_{pw}(T_i) + m_t c_{pt}(T_i)}{m_p}\right) \frac{A_c}{A'_c} \frac{I_2}{I'_2} (T_m - T_i). \tag{10}$$

Kravvaritis et al. [17] proposed the thermal delay method to obtain the change of the effective heat capacity ($c_{p,eff}$) of the PCM with the temperature, considering the temperature difference between the PCM and the reference for the same time intervals. Measurement process time and errors could be significantly reduced using this method, since it is not required to identify the phase change zones using the first derivative or fitting the data obtained during the test. The authors proposed the calculation of the $c_{p,eff}(T)$ using the same procedure of the T-history method, considering the differences in time when the reference fluid and the PCM are at the same temperatures T_i and T_{i+1}, according to is shown in Figure 4a. The areas under the cooling curves were calculated using the following expressions:

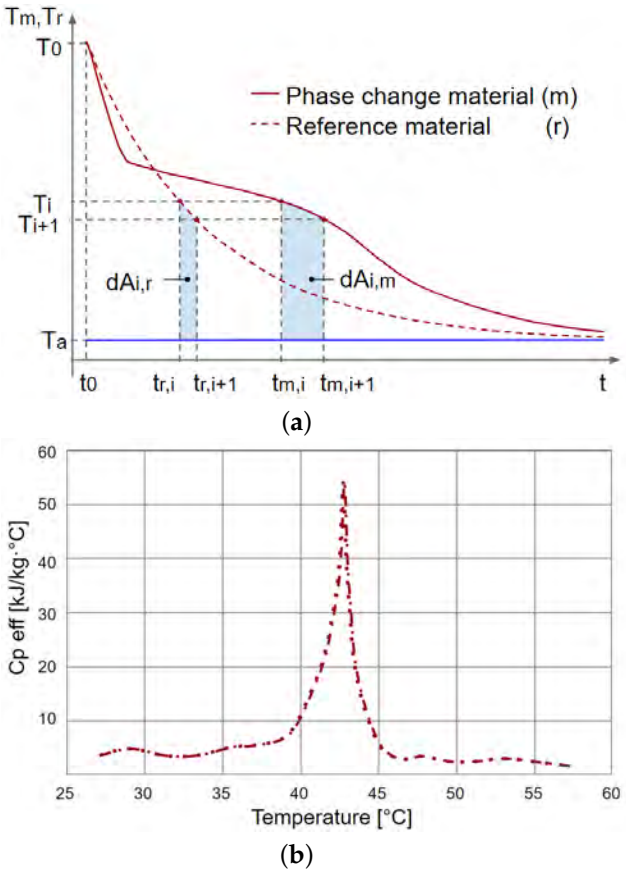

Figure 4. (**a**) Schematic representation of the effective thermal capacity calculation method; (**b**) Effective thermal capacity vs. temperature. Adapted from [17].

$$\mathrm{d}A_{i,m} \cong \left(T_i + T_{i+1} - 2T_a\right)\left(t_{m,i+1} - t_{m,i}\right)/2 \tag{11}$$

$$\mathrm{d}A_{i,r} \cong \left(T_i + T_{i+1} - 2T_a\right)\left(t_{r,i+1} - t_{r,i}\right)/2. \tag{12}$$

The following expression is obtained for $c_{p,eff}(T)$:

$$c_{p,eff}(T) = M\frac{\mathrm{d}A_{i,m}}{\mathrm{d}A_{i,r}} - N \tag{13}$$

where:

$$M = \left(\frac{m_w c_{pw} + m_t c_{pt}}{m_p}\right)\frac{A_c}{A_c'} \tag{14}$$

$$N = \frac{m_t}{m_p}c_{pt}. \tag{15}$$

Researchers show that the results obtained with the proposed method are consistent with measurements made with a DSC. When the results are plotted, a function of the $c_p - T$ can be obtained as shown in Figure 4b, in which an increase in the function in the phase change region is exhibited.

2.3. Determination of Thermal Properties Using the T-Melting CHF Method

Another method developed for the determination of PCM thermophysical properties such as the melting point, latent heat of fusion, thermal conductivity and specific heat capacity in both phases was developed by Yang et al. [34]. This method is based on the solution of the Stefan's problem under constant heat flux (CHF) boundary conditions. For experimental measurement, the temperature of a PCM sample must be monitored during the fusion process, while a constant heat flux condition is applied at one of the boundaries, so the process is commonly known as "T-melting CHF".

Some of the advantages of this method are the short experimentation time because only the fusion process is analyzed, the assembly is relatively simple since—(i) the constant heat flow condition can be achieved by applying constant heating power; (ii) standard reference samples are not required as in other tests, and most importantly; (iii) multiple properties can be determined in a single test. The theoretical principle that describes the phase change problem in materials is known in the literature as Stefan's problem, which is characterized by having a moving boundary whose position is unknown a priori. For the problem under constant heat flow conditions, there is no exact solution. Nevertheless, some approximate solutions have been developed for the Stefan's one-dimensional (1D) problem. Government equations for the phenomenon are derived by considering the melting problem of a solid state PCM slab with width W, which is at an initial temperature equal to that of the phase change (T_m). When a constant heat flow is applied to the left, the PCM begins to melt and two zones are generated: a liquid and solid region with the interface between them, which is designated as $s(t)$, which moves to the right as the solid region melts, as is illustrated in Figure 5a. The governing equation of this problem (Equation (16)) has the drawback that both the temperature distribution $T(x,t)$ and the location of the liquid-solid interface $s(t)$ are unknown.

$$\frac{\partial\left(\rho_l c_{p,l} T\right)}{\partial T} = \frac{\partial}{\partial x}\left(k_l \frac{\partial T}{\partial x}\right) \qquad 0 \le x \le s(t),\ t > 0. \tag{16}$$

The CHF method uses the approximate solution of the quasi-static fusion model to simplify the governing equations. It is assumed that natural convection in the liquid is negligible and therefore only conduction is considered, and it is assumed that the properties of the PCM are not temperature dependent and only depend of the phase [34]. So introducing the constant heat flux

boundary condition on the left side of the wall, we can obtain the expressions for the interface and the temperature distribution:

$$s(t) = \frac{q'' t}{\rho_l \Delta H} \tag{17}$$

$$T = \frac{q''}{k_l}[s(t) - x] + T_m \qquad 0 \le x \le s(t), \quad t > 0. \tag{18}$$

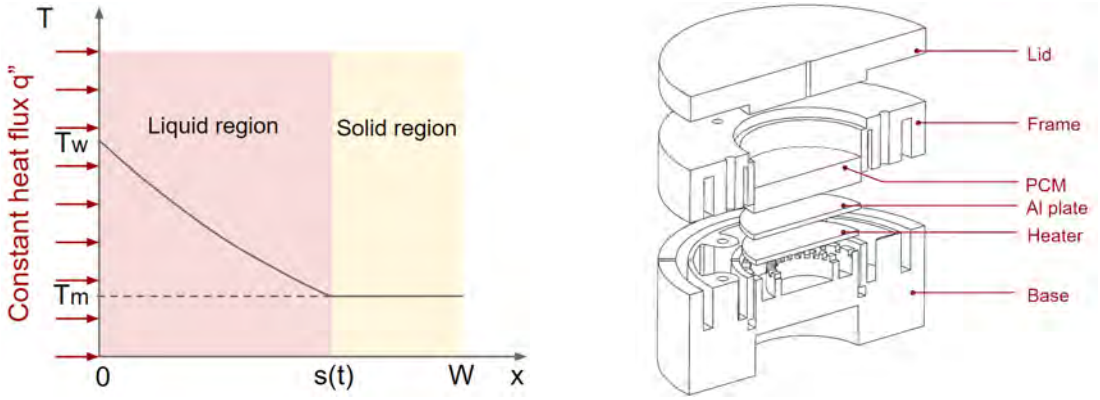

(**a**) (**b**)

Figure 5. (**a**) Schematics of the 1D single-phase melting problem under constant heat flux (CHF) condition; (**b**) Cross-sectional view of the schematic of the experimental setup. Adapted from [34].

The approximate solution obtained in a dimensionless way used by the authors as a theoretical formula for determining the thermophysical properties of PCM are expressed in Equations (19) and (20).

$$\bar{s} = Ste \cdot Fo \tag{19}$$

$$\Theta = \bar{s} - \bar{x}, \tag{20}$$

where $Fo = k_l t/\rho_l c_{p,l} W^2$; is the Fourier number (dimensionless time); $\Theta = (T - T_m)/\Delta T_c$ is the dimensionless temperature; $Ste = c_{p,l}\Delta T_c/\Delta H$ is the Stefan number; $\Delta T_c = q'' W/k_l$ is the characteristic temperature difference; $\bar{s}$ and $\bar{x}$ are the dimensionless form of s and x respectively.

The test module is made up of six main parts, as shown in Figure 5b. The base, frame and lid form a container to store the sample. The container, for insulation purposes, must be a material with low thermal conduction, the original proposed module was built in PTFE, with a thermal conductivity of 0.24 W/m-K and a melting point of 326.8 °C, which constitute optimal characteristics for testing in a wide range of low temperature applications.

A heating power must be supplied to the heater which is monitored through the supplied voltage and current. Two thermocouples are sandwiched between the aluminum plate and the top of the heater and their average value is recorded as the monitoring temperature (T_{mon}) as seen in Figure 6a. The temperature at the top of the aluminum plate in contact with the PCM (which acts as the heating wall) can be estimated using the Fourier law of conduction:

$$T_w = T_{mon} - \frac{q_{hs} L_{Al}}{A_{hs} k_{Al}}, \tag{21}$$

where $L_a l$ y $k_a l$ are the thickness and thermal conductivity of the Al plate respectively, and $A_h s$ is the sectional area of the heat source. Assuming no heat losses in the test module, Figure 6b schematically represents a typical monitoring temperature curve (T_{mon}). The process can be divided in three sections: before, during, and after melting section. T_{refl} are the reflection points at which the PCM begins and

ends to melt at times t_1 and t_2, respectively. According to the model, the melting point of the PCM can be obtained using the following equation:

$$T_m = T_{refl,1} - \frac{q_{hs} L_{Al}}{A_{hs} k_{Al}}. \tag{22}$$

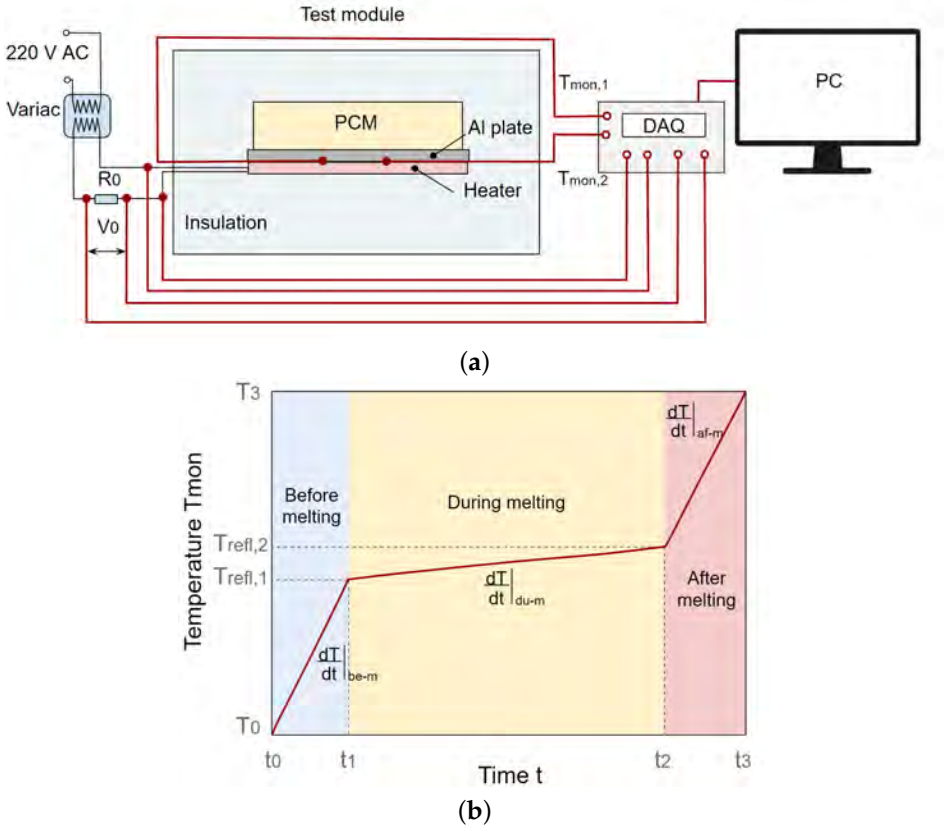

Figure 6. (**a**) Schematic of the measurement device; (**b**) Schematics of a temperature response under constant heating power q_{hs}. Adapted from [34].

Considering each one of the sections individually, that is, before, during and after the phase change, it is possible to obtain relations for $c_{p,s}$, $c_{p,l}$ and it also allows calculating the amount of heat absorbed by the PCM in form of latent heat, so ΔH can be obtained.

Theoretically the wall temperature increases almost linearly with time, so in the phase change zone:

$$\left.\frac{dT}{dt}\right|_{du-m} = \frac{q_m / A_{hs}}{\rho_{l,PCM} k_{l,PCM} \Delta H}. \tag{23}$$

Therefore, previously knowing the liquid density (ρ_l), it is possible to calculate the thermal conductivity k_l.

The CHF method must satisfy some restrictions to guarantee the accuracy of the measurements, (i) the 1D fusion process requires that in the molten liquid region of the PCM sample there is no Rayleigh-Bénard convection, therefore, $Ra < Ra_c$; (ii) the quasi-stable state approximation is appropriate for cases with a small Ste number. So $Ste < Ste_c$; (iii) the heat flux q'' is below a critical value q''_c.

3. Experimental Determination of Thermal Properties

This section presents the experimental equipment used, materials, methods and values obtained for the properties of the PCM analyzed with the different methods.

3.1. Materials

For the experimental validation of the methods studied in this research, experimental characterization of 2 commercial paraffins RT45 and RT55 distributed by Rubitherm® [35] was carried out. The purpose in the present work was to study the specific case of widely used, commercially available materials, of the class of paraffins. These two materials were chosen because they are in the temperature range for a wide applications in thermal energy storage, as sanitary water and solar heating. Furthermore, the supplier has RAL certification, which makes them suitable materials to compare with the experiments proposed here.

The thermal properties indicated by the manufacturer are listed in Table 1.

Table 1. Thermal properties of paraffin waxes RT45 and RT55 given by manufacturer's datasheet [35].

Properties	RT45	RT55
Tm (main peak) [°C]	45	55
Heat storage capacity [kJ/kg]	160	170
Specific heat capacity [kJ/kg·K] [1]	2	2
Density liquid [kg/m^3] (at 15 °C)	770	770
Density solid [kg/m^3] (at 80 °C)	880	880
Thermal conductivity [W/m·K] [1]	0.2	0.2

[1] Both phases.

3.2. Determination of Thermal Properties with T-History

The samples were arranged in three test tubes with 15 mm internal diameter, 175 mm length and 1.2 mm thick wall, which were filled up to 80% of the total volume of the tube, three test tubes were used in each test, in one of these, distilled water was used as reference and the others two were filled with samples of the same type of PCM. The test tubes were sealed with rubber plugs, through which the thermocouples were passed (see Figures 2 and 7).

The initial temperatures of the process were defined according to each material tested, so the thermostatic bath was programmed at a temperature between 10 °C and 15 °C above the melting temperature reported by the manufacturer. The specimens were immersed until the thermal equilibrium between the samples and the hot medium was reached. temperature was monitored using an AT4208 digital temperature meter and K-type thermocouples, the mean mass of each group of samples was around 12 g. Once the temperatures inside the specimens were stabilized and homogenized, both the samples and reference were transferred to insulated containers of EPS, as is shown in Figure 7, in order to avoid convective effects and satisfy the condition of $Bi < 0.1$.

Results of the cooling curves for both the reference and the PCM samples are used to estimate the thermophysical properties. With the aim of determining the start and end regions of the phase change, Figure 8 shows the cooling curves and inflection points calculated with the numerical first derivative of the temperature curve in the PCM resulting from the T-history.

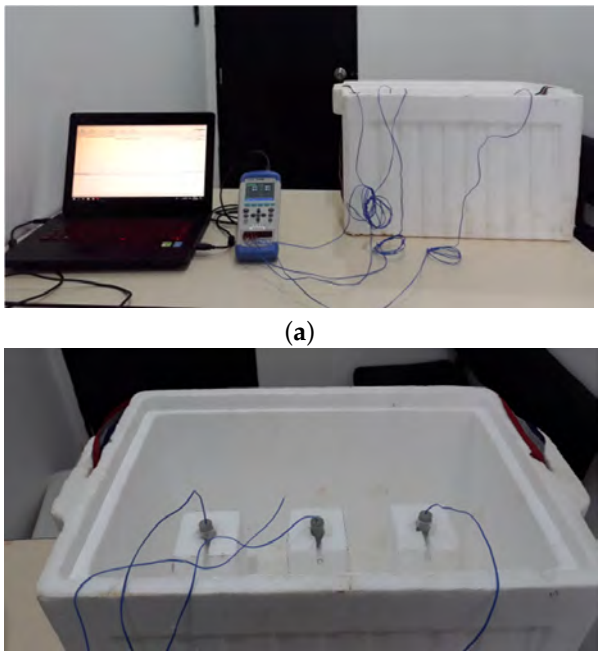

(**a**)

(**b**)

Figure 7. (**a**) Experimental setup implementing the scheme of Figure 2; (**b**) Insulation of the test specimens.

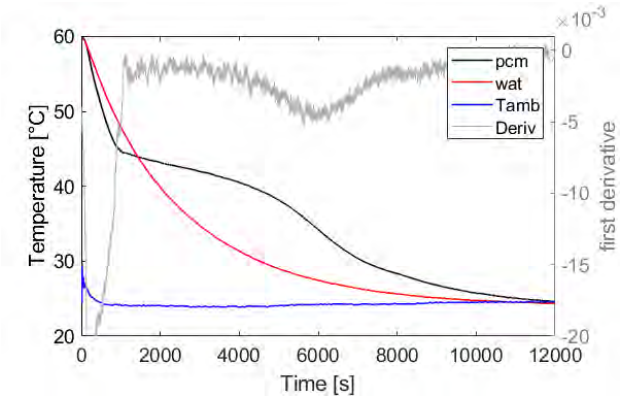

(**a**)

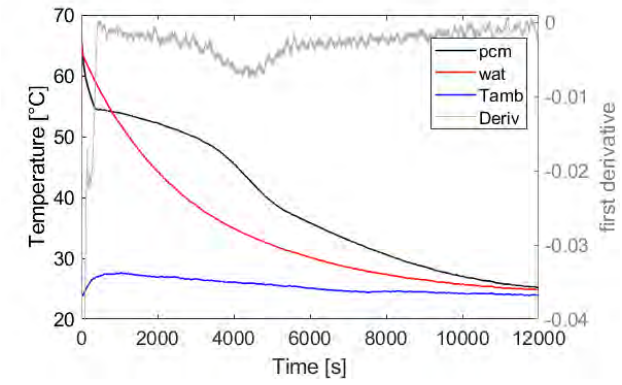

(**b**)

Figure 8. Resulting cooling curves (**a**) RT45; and (**b**) RT55. pcm: Sample of PCM. wat: reference test tube (water). Tamb: ambient temperature: Deriv: numerical derivative of sample temperature.

Ten samples of each PCM tested were made and results are condensed in Tables 2 and 3.

Table 2. Determination of thermal properties with T-history to RT45 paraffin.

Data	T_l [°C]	T_s [°C]	H_m [kJ/kg]	$c_{p,l}$ [kJ/kg]	$c_{p,s}$ [kJ/kg]
Mean value	44.33	35.95	166.72	2.22	4.35
St. deviation	0.14	0.73	5.63	0.14	0.15
Manufacturer value [35]	46	40	160	2	2
Disagreement %	3.21	13.05	1.28	11.32	117.69

Table 3. Determination of thermal properties with T-history to RT55 paraffin.

Data	T_l [°C]	T_s [°C]	H_m [kJ/kg]	$c_{p,l}$ [kJ/kg]	$c_{p,s}$ [kJ/kg]
Mean value	54.51	42.82	168.30	2.43	5.36
St. deviation	0.07	0.75	3.29	0.34	0.21
Manufacturer value [35]	57	56	170	2	2
Disagreement %	4.37	23.54	1.01	21.91	168.16

Values of effective thermal capacity ($c_{p,eff}$) were estimated from Equation (13), using the cooling curves obtained experimentally for PCM RT45 and RT55 from T-history method. Results for a data set are presented in Figure 9. Note that the peak in the graph is due to the amount of energy it would take to increase the temperature by one degree Celsius, which is higher in the phase change zone due to the energy required by latent heat.

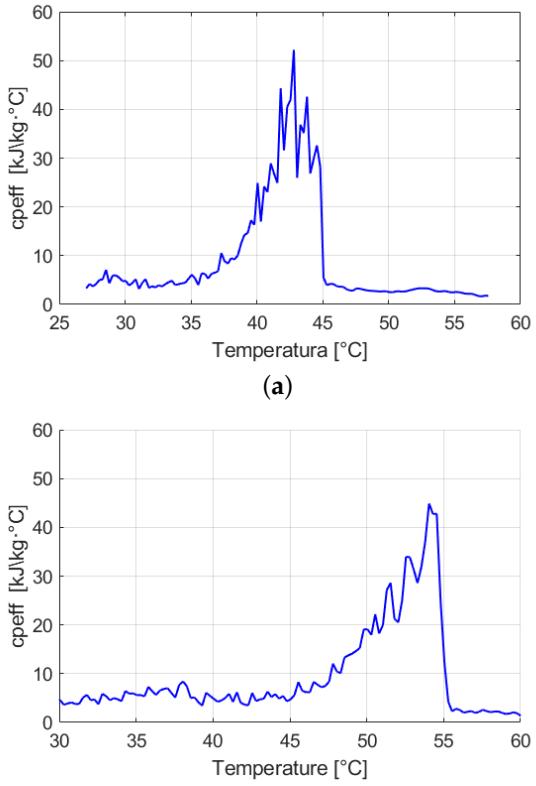

Figure 9. Effective thermal capacity in terms of the temperature evaluated by the T-history method (**a**) RT45; and (**b**) RT55.

3.3. Determination of Thermal Properties with T-Melting CHF

The measuring device was manufactured replicating the model proposed by Yang et al. [34], it was built by 3D printing on acrylonitrile butadiene styrene (ABS), which has a thermal conductivity of 0.17 W/m·K and a maximum use temperature of 100 °C, these characteristics satisfy the requirements

for the evaluation of the PCM. Figure 10a,b show the structure of the test module, the heat source used shown in Figure 10c and has a 50 mm diameter with a thickness of 2 mm, a resistance of 616 Ω and a maximum power 70 W heating circuit. The heat flow was supplied by an alternating current transformer (Variac), the temperature was monitored by the APPLENT AT4208 digital meter and two K-type thermocouples.

(**a**) (**b**) (**c**)

Figure 10. Elements for the implementation of the T-melting CHF method. (**a**) Device assembly; (**b**) top view of base, frame, and Cap; (**c**) electric heating resistance.

PCM RT45 and RT55 were evaluated following the methodology proposed by Yang et al. [34]. A PCM conductivity value of 0.2 W/m·°C is take as the reference according to the information provided by the supplier and samples with a thickness of 0.005 m were tested, so the critical heat flux q_c'' is 2000 W/m^2, all tests were performed with a heat flux below the critical heat flux. Likewise, the Rayleigh number for each test is below the limit value $Ra_c = 2.72 \times 10^4$. Therefore, heat transfer in the tests by conduction is guaranteed. measurements were made with a Ste greater than 0.2 but less than 0.5, so the results are expected to present errors of less than 16.7%, according to what was reported by the original authors. The results obtained are presented in Tables 4 and 5.

Table 4. Determination of thermal properties of RT45 with T-melting method.

Data	T_m [°C]	k [W/m]·°C]	H_m [kJ/kg]	$c_{p,l}$ [kJ/kg]	$c_{p,s}$ [kJ/kg]
Mean value	45.72	0.2351	157.1651	17.5405	2.1590
St. deviation	–	0.0258	5.2184	5.5266	0.1233
Manufacturer value [35]	–	0.2	160	2	2
Disagreement %	–	17.57	1.77	777.03	7.95

Table 5. Determination of thermal properties of RT55 with T-melting method.

Data	T_m [°C]	k [W/m]·°C]	H_m [kJ/kg]	$c_{p,l}$ [kJ/kg]	$c_{p,s}$ [kJ/kg]
Mean value	57.78	0.2022	175.2850	24.4099	2.6226
St. deviation	–	0.0106	7.4692	1.6386	0.1353
Manufacturer value [35]	–	0.2	170	2	2
Disagreement %	–	1.10	3.11	1120.5	31.13

From the results of the experimental measurements, large deviations for the specific heat capacity c_p are evident, especially for the liquid phase, whose relative deviation reaches unacceptable deviations. This error was due to the simplifications that made the method experimentally practical, by neglecting the convective effects in the liquid phase. Although the insulation in the test module can be guarantee, this error cannot be attributed to the loss of heat in the measurement device, because the specific heat in solid phase is in agreement whit the expected value.

3.4. Density Determination

The value of the density of a material is obtained through the relationship between the mass and its volume. To obtain the value of the density of the samples analyzed, 10 mL graduated pipettes previously sealed at the lower tip were used, which were weighed on a 0.1 mg precision balance to record their mass. Subsequently, the paraffin samples were melted at a temperature higher than the melting temperature and the pipettes were filled. Once the sample was at room temperature, its initial volume (V_0) was determined as is shown in Figure 11, density in the solid state could be calculated by means of the relation mathematics between them. In an analogous way, the density calculation for the liquid phase was performed the test tube with the PCM sample was introduced in a thermal bath, at a temperature 10 °C above its melting temperature and proceeded to read the new volume (V_f). 5 repetitions of each sample of the PCM evaluated were performed, the averaged values are presented in Table 6.

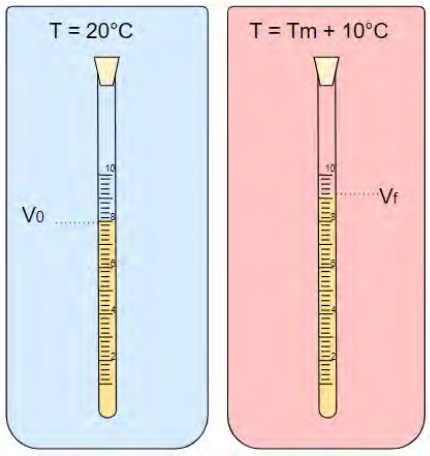

Figure 11. Schematics of the procedure to calculate the density.

Table 6. Density results.

Material	ρ_s [kg/m^3]	ρ_l [kg/m^3]	Manufacturer Value
RT45	873.3	768.5	880/770
RT55	856.6	789.4	880/770

3.5. Determination of Thermal Properties by DSC

The equipment used was the Discovery series DSC 250 (manufactured by TA Instruments, Newcastle, DE, USA) and is coupled to a cooling system (RCS90) that allows experimental test in a temperature range between −90 °C up to 550 °C. One of the most important aspects is to determine which is the heating/cooling ramp to be used during the tests, because it could affect the phase change enthalpy values and the specific heat curvesobtained in each case. For the experimental evaluation, the ASTM D4419 standard for measurement of transition temperatures of petroleum waxes by DSC was used as a guide, the recommended rate of 10 °C/min ± 1 °C/min up to 20 °C ± 5 °C beyond melting. However, following the recommendation of RAL, rates of 20, 10, 5, 1, 0.5 °C and 0.3 °C/min were additionally included to perform the experimental evaluation. Figure 12a shows the heat flux signal (mW/g) obtained from a DSC test for a heating rate of 5 °C/min. Variation of the heat flow over temperature identifies the region where the phase transition occurs. The tests were performed in dynamic mode, that is, using a constant speed for the heating and cooling ramps between the initial and final temperatures selected for each test as is shown in Figure 12b.

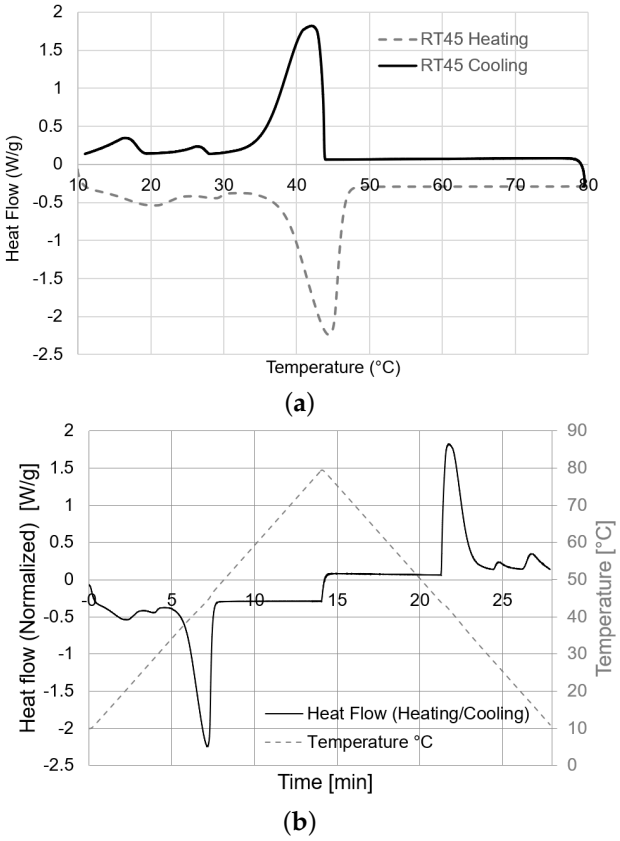

Figure 12. (**a**) Differential scanning calorimetry (DSC) curve; (**b**) Typical DSC response when performing a dynamic mode, heating and cooling.

The RT45 and RT55 paraffins were subjected to heating and cooling programs using the DSC, finding that the values for the phase change enthalpy of the RT45 paraffins range from 137 to 166 kJ/kg, while for the RT55 they range from 137 to 145 kJ/kg, these values are highly sensitive to the test speed, as is shown in Figure 13, in which the results of the fusion enthalpies are presented after analyzing the DCS tests for different cooling rates. In this figure, it can be observed that as the cooling speed decreases, the start of the phase change moves towards a higher temperature value. It can be seen that for cooling speeds in the DSC of 20 °C/min, the start of the phase change is close to 43.6 °C with an enthalpy of solidification of 144 kJ / kg on average, while for speeds of 1, 0.5 and 0.3 °C/min the start of the phase change is closer to 44.6 °C with an average solidification enthalpy value of 152 kJ/kg. For the heating process the results were a little lower, finding a fusion enthalpy of 142 kJ/kg, an average melting start temperature of 38.1 °C.

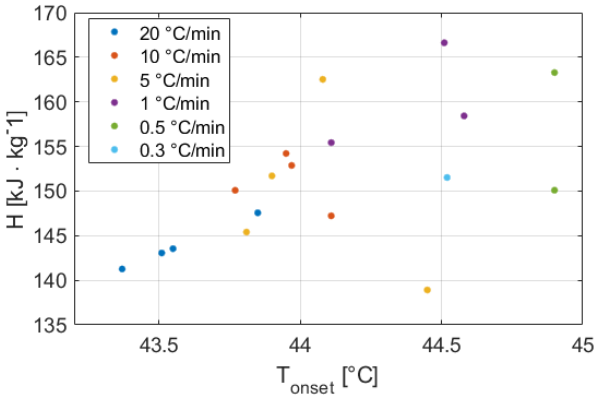

Figure 13. Dispersion of energy storage data for RT45 paraffin in the cooling process.

This result can be evidenced with an Enthalpy-Temperature diagram like those shown in Figure 13, this representation was proposed by Marín et al. [14], which is useful for the analysis of energy accumulators. As is presented in Figure 14a the phase change process for the studied samples presents hysteresis, which explains why the start of the phase change are different for both cooling and heating. It can be seen that the slopes of the initial and final sections represent the values of the specific heat in the solid and liquid states, it is also to be expected that, if the substance were pure, the phase change will appear as a vertical line at a value of specific temperature, but for materials such as paraffins, the phase change occurs in a range from a temperature T_{m1} to a temperature T_{m2}. Figure 14a also shows that the H_m value corresponds to the energy required for the phase change, while the manufacturer in this case reports the H_s value (see Figure 14a), which is between the temperatures of 37 °C to 52 °C for PCM RT45 and 48 °C to 63 °C for PCM RT55, respectively. This value of H_s represents a combination of latent heat and sensible heat in the indicated temperature ranges. The average values found for RT45 at different rates are presented in Table 7.

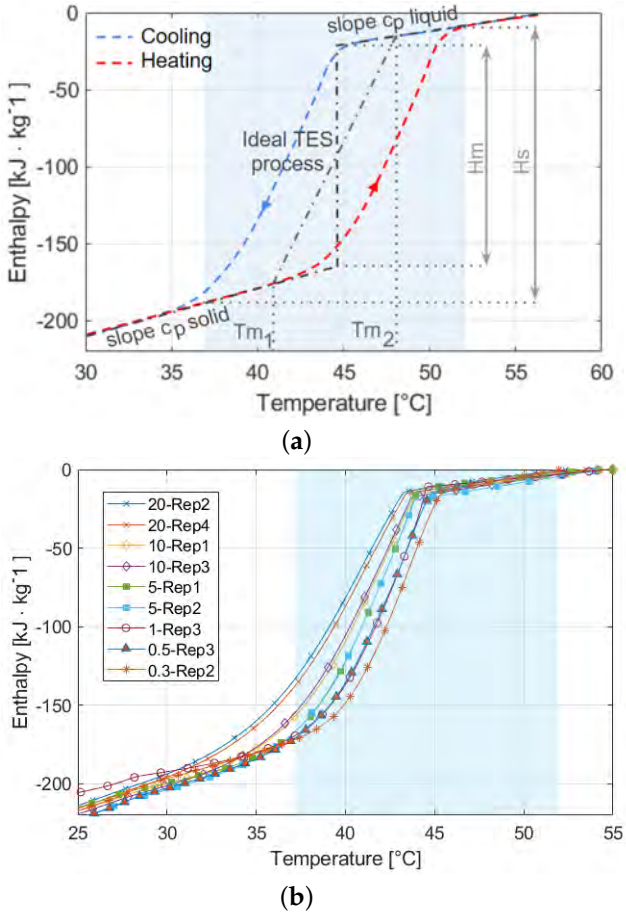

Figure 14. (**a**) Behavior of a PCM after heating and cooling process; (**b**) Enthalpy-temperature curve for the experimental PCM RT45 in cooling process.

Table 7. Experimental DSC results in range given by manufacturer.

Cooling Ramp	Peak Temp	H_s [kJ/kg]
20 °C/min	39.6 °C	136.67
10 °C/min	41.2 °C	154.98
5 °C/min	42.1 °C	165.49
1 °C/min	43.9 °C	167.37
0.5 °C/min	44.3 °C	164.45
0.3 °C/min	44.5 °C	170.63

The manufacturer's reported value for the stored heat for the RT45 is 160 ± 7.5%, so the speed of 20 K/min do not adjust to the values in the datasheet. On the other hand, with temperature rates below 10 K/min, the measurements are in agreement with the datasheet of the supplier. In Figure 14b. Some of the results obtained for the RT45 sample are presented, the difference between the results obtained in relation to the cooling rates used in the DSC is evident, it can be seen that as the cooling rate becomes lower, the phase change occurs in a narrower range of temperatures. In the temperature range indicated by the manufacturer, the stored energy corresponds to a sum of sensible heat and latent heat. It is also seen that for high cooling speeds, part of the latent heat would be no longer quantified in the specified phase change interval. Therefore, it is concluded that the speed range indicated by ASTM D4419-90 is not recommended for this type of materials.

The specific heat curves obtained are presented in Figure 15a, where it can be seen that as the cooling/heating rate is decreased, the value of the resulting maximum peak becomes greater, as long as samples with the same amount of mass are tested. The results are consistent with that reported by Mehling et al. [36], which are presented in Figure 15b, where it is shown that for equal heating rates, but with higher mass a lower peak value is reached.

Results obtained for the PCM RT45 in Figure 15a, show how for the peak value of c_p becomes greater as the cooling rate decreases in the DSC, in which 5.3 mg of the sample were used. However, for the speed of 0.3 K/min the mass used was 8.8 mg and it can be seen how the peak value of the specific heat does not exceed the value reached with a higher speed of 1 K/min. The variability of these results demonstrates the importance of having a unified standard for measurements to be carried out in PCMs using the DSC. Furthermore, these rate speeds are rather different from those recommended in ASTM standards.

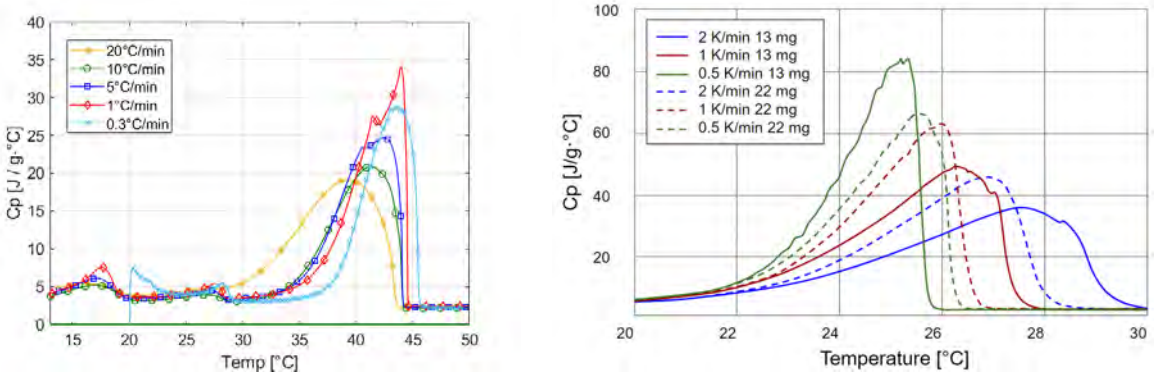

(**a**) (**b**)

Figure 15. (**a**) Specific heat capacity of the PCM RT45 varying heating rates and sample mass; (**b**) Results for the heat capacity of a PCM varying heating rates and sample mass, adapted from [36].

4. Discussion

To compare the results obtained between the T-history method and the DSC, the cooling rate of the PCM samples is calculated from the T-history. It is represented in Figure 16, which shows that for both RT45 and RT55, the cooling rate vary in some sections, but in general terms they are lower than 0.2 °C/min on average, which represents cooling rates slightly lower than those evaluated by DSC.

Figure 17 shows one of the greater advantages of T-history method over DSC and its use in thermal energy storage applications: It allows to evaluate a representative sample of non-pure PCM in conditions close to those usually presented in actual practice. Other advantage is that when insulated PCM samples are evaluated, lower cooling speeds are obtained, and in the general case of DSC equipment that is cooled by nitrogen, noise signals are induced at low cooling speeds, which complicates the estimation of the specific heat.

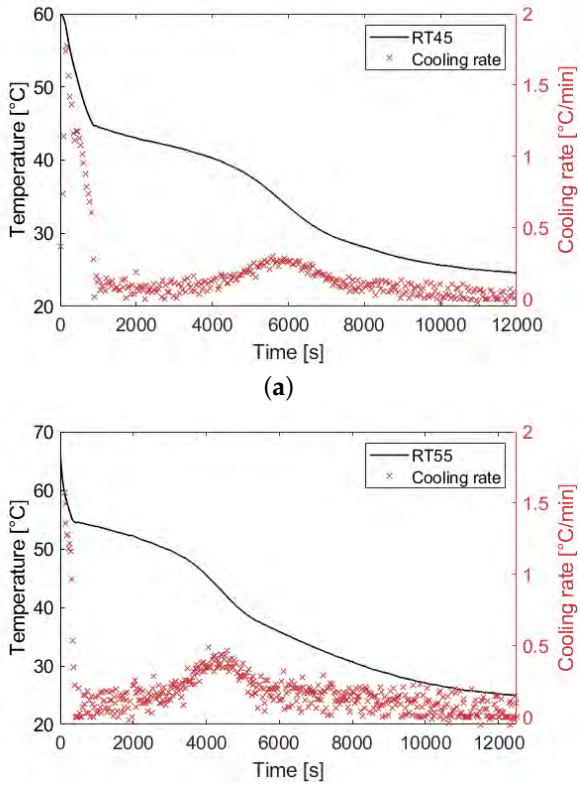

Figure 16. Heating rate from T-history test (**a**) RT45; (**b**) RT55.

Results are compared in an Enthalpy-Temperature diagram in Figure 17 When comparing the amount of heat stored in the range given by the manufacturer, an average H_s value of 159.74 kJ/kg was obtained, which shows the consistency between the results obtained by the T-history with respect to those obtained by DSC.

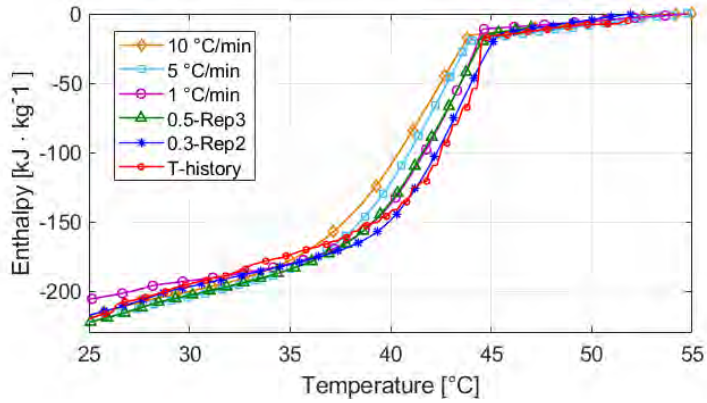

Figure 17. Enthalpy-Temperature comparison between DSC and the T-history method.

Figure 18 presents the superimposed curves between the results obtained by the DSC, those calculated with the T-history method, and the equations proposed by Kravvaritis et al. [17] for the effective heat capacity. Correspondence is evident between the results; it was expected that at much lower cooling rates in the T-history method than in the DSC, a higher peak would be obtained.

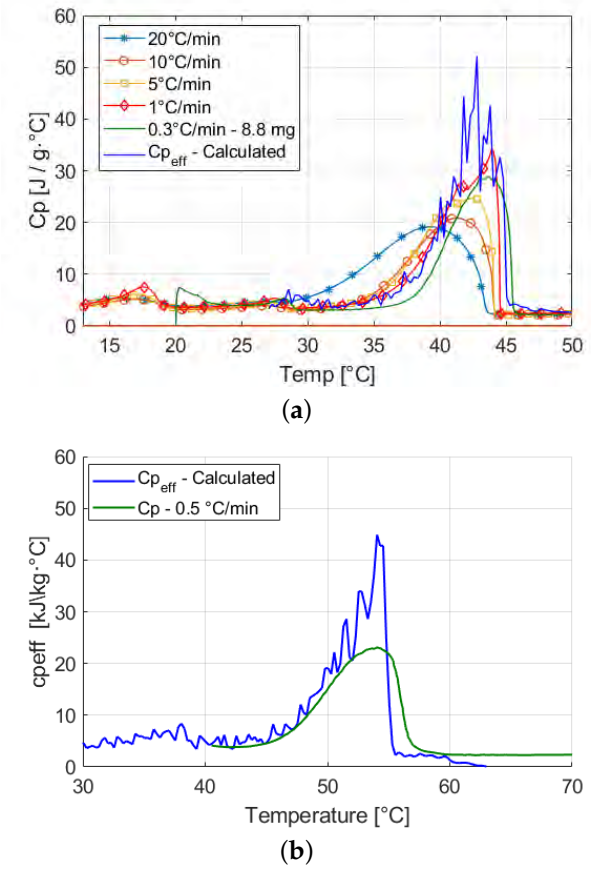

Figure 18. (Comparison of cp results between the $c_{p,eff}$ and the DSC method (**a**)) RT45; (**b**) RT55.

When comparing the conventional, unconventional experimental results and the values reported in the manufacturer's data sheet, discrepancies are evident (Table 8), among which it is highlighted that: (i) values of the phase change temperatures and enthalpies of fusion/solidification can be obtained by the T-history and T-melting methods. (ii) For the calculation of the conductivity, results obtained by the T-melting method show good correspondence with the values presented by the manufacturer. Colla et al. [37] experimentally determined the conductivities of the RT45 and RT55 paraffins using an instrument based on the hot disk technique, (ThermTest TPS 2500s) to measure thermal conductivity. The instrument operates in transient plane source mode using a Kapton insulated disk sensor in order to be thermally neutral. Values obtained experimentally by these authors for the RT45 paraffin was 0.2415 W/m·K while for the RT55 it was 0.3336 W/m·K. Therefore, when results obtained and provided by the manufacturer of 0.2 W/m·K and those calculated by the T-melting CHF are compared, greater differences are found. Nevertheless, the T-melting CHF method allows obtaining a general estimate of the property. (iii) The stored energy can be determined by the T-history in the evaluated range, while with the T-melting CHF method an estimated phase change value is obtained that is consistent with the results obtained by the DSC. (iv) the specific heat in liquid phase calculated by the CHF method differs from that reported by the manufacturer, which can be justified not only by a poor insulation of the experimental module, as mentioned by [34], but rather by the simplification of the model, which does not consider the convective effects in the liquid phase. so it is not recommended for the estimation of this property. However, the calculated solid phase specific heat is a good overall estimate of the property. Although the manufacturer provides the same value for the specific heat in both phases for its possible proximity and ease of handling, it is clear that the value of this property is lower in the liquid phase than in the solid phase, this is in agreement with the results obtained from calorimetry, which is consistent with the results found with the T-history method.

Table 8. Comparison of the thermal properties measured of RT45, [a] Rate 0.5 K/min, [b] Cooling, [c] H_m.

Measurement Method	T-History	T-Melting	Man. Value [35]	Exp. Density	DSC [a]	Literat. [37]
T_m (°C) [b]	44.60	45.72	45	–	44.3	–
K (W/m·K)	–	0.23	0.2	–	–	–
H_s (kJ/kg)	164.45	157.16[c]	160	–	164.45	–
$c_{p,l}$ (kJ/kg)	2.22	17.54	2	–	1.26	–
$c_{p,s}$ (kJ/kg)	4.35	2.15	2	–	2.25	0.2415
ρ_l (kg/m^3)	–	–	770	768.5	–	–
ρ_s (kg/m^3)	–	–	880	873.3	–	–

Finally, it is evident that the data provided by the manufacturer serves as a general guide for its use in thermal energy storage applications. However, it is advisable to determine the thermal properties under the same experimental conditions in which they will be used. Although the need of standards for the determination of each of the properties of phase change materials is evident, it is understandable that this remains a technical challenge since they can be affected by the inherent characteristics of the process in which it will be used. However, when it is required to guarantee the equilibrium values, it is required to proceed in accordance with what was reported by Gschwander et al. [9], in which a very slow velocities for heating and cooling are recommended.

5. Conclusions

The performance of two low cost unconventional methods (T-history and T-melting CHF) were evaluated to estimate the thermal properties in PCM. Obtained results were compared with the values reported by the manufacturer and those obtained by DSC for two different commercial PCM. Despite the sensitivity to the mass of the sample and the rate of cooling/heating and the issues presented for non-homogenous materials, DSC measurements are taken as the reference, since it is the most widely used method for the determination of thermophysical properties in materials, including PCMs.

Results obtained with the T-history method present very good agreement for the stored or released energies. However major discrepancies were found for $c_{p,liq}$ with the T-melting CHF method and for $c_{p,sol}$ with the T-History method. However, both methods can be used as a preliminary estimation of the property if it is unknown a priori. The T-melting method has clear benefits for the determination of thermal conductivity. The determination of $c_{p,liq}$ with T-melting is not recommended due to the simplifications of the method concerning the convection effects. The accuracy of both T-history and T-melting methods can be improved by reducing the heat losses of the devices. Results obtained in this work show that the use of low-cost methods is a reasonable alternative to estimate the thermal properties of the PCM if a good combination of the techniques is implemented.

Author Contributions: Conceptualization, A.M., M.C., C.C. and I.A.; Data curation, A.M., M.C., C.C. and I.A.; Formal analysis, A.M., M.C., C.C. and I.A.; Funding acquisition, A.M., M.C., C.C. and I.A.; Investigation, A.M., M.C., C.C. and I.A.; Methodology, A.M., M.C., C.C. and I.A.; Project administration, A.M., M.C., C.C. and I.A.; Resources, A.M., M.C., C.C. and I.A.; Supervision, A.M., M.C., C.C. and I.A.; Validation, A.M., M.C., C.C. and I.A.; Visualization, A.M., M.C., C.C. and I.A.; Writing–original draft preparation, A.M., M.C., C.C. and I.A.; Writing–review and editing, A.M., M.C., C.C. and I.A. All authors have read and agreed to the published version of the manuscript.

Funding: This research has been partially funded by Universidad Del Norte with his PhD Scholarship Contract Identification Number: UN-OJ-2013-22063, the Colombian Administrative Department of Science, Technology and Innovation-COLCIENCIAS Scholarship Call No 727 of 2015 and through the program “es tiempo de volver”.

Conflicts of Interest: The authors declare no conflict of interest.

Abbreviations

The following abbreviations are used in this manuscript:

CHF Constant Heat Flux
DSC Differential Scanning Calorimetry
PCM Phase Change Materials

MWCNT	multiwall carbon nanotubes
NEPCM	Nano-Enhanced PCM
TES	Thermal Energy Storage

References

1. Faraj, K.; Khaled, M.; Faraj, J.; Hachem, F.; Castelain, C. Phase change material thermal energy storage systems for cooling applications in buildings: A review. *Renew. Sustain. Energy Rev.* **2020**, *119*, 109579. [CrossRef]
2. Carmona, M.; Palacio, M. Thermal modelling of a flat plate solar collector with latent heat storage validated with experimental data in outdoor conditions. *Sol. Energy* **2019**, *177*, 620–633. [CrossRef]
3. Khan, M.M.A.; Saidur, R.; Al-Sulaiman, F. A review for phase change materials (PCMs) in solar absorption refrigeration systems. *Renew. Sustain. Energy Rev.* **2017**, *76*, 105–137. [CrossRef]
4. Gschwander, S.; Lazaro, A.; Cabeza, L.F.; Günther, E.; Fois, M.; Chui, J. Development of a test standard for PCM and TCM characterization part 1: Characterization of phase change materials. *IEA Rep. A* **2011**, *2*, 1–46.
5. Barreneche, C.; Pisello, A.L.; Fernández, A.I.; Cabeza, L.F. Experimental Methods for the Characterization of Materials for Latent Thermal Energy Storage. In *Recent Advancements in Materials and Systems for Thermal Energy Storage*; Springer: Cham, Germany, 2019; pp. 89–101.
6. Barreneche, C.; Solé, A.; Miró, L.; Martorell, I.; Fernández, A.I.; Cabeza, L.F. Study on differential scanning calorimetry analysis with two operation modes and organic and inorganic phase change material (PCM). *Thermochim. Acta* **2013**, *553*, 23–26. [CrossRef]
7. Mehling, H.; Barreneche, C.; Solé, A.; Cabeza, L.F. The connection between the heat storage capability of PCM as a material property and their performance in real scale applications. *J. Energy Storage* **2017**, *13*, 35–39. [CrossRef]
8. Günther, E.; Hiebler, S.; Mehling, H.; Redlich, R. Enthalpy of phase change materials as a function of temperature: Required accuracy and suitable measurement methods. *Int. J. Thermophys.* **2009**, *30*, 1257–1269. [CrossRef]
9. Gschwander, S.; Haussmann, T.; Hagelstein, G.; Barreneche, C.; Ferrer, G.; Cabeza, L.; Hennemann, P. Standardization of PCM characterization via DSC. In Proceedings of the SHC 2015 International Conference on Solar Heating and Cooling for Buildings and Industry, Istanbul, Turkey, 2–4 December 2015; pp. 2–4.
10. Phase Change Materials 2018 Quality Assurance RAL-GZ 896, 2018. Available online: https://www.pcm-ral.org/pdf/RAL_GZ_896_Phase_Change_Material_Edition_March_2018.pdf (accessed on 5 June 2020).
11. Ferrer, G.; Barreneche, C.; Solé, A.; Martorell, I.; Cabeza, L.F. New proposed methodology for specific heat capacity determination of materials for thermal energy storage (TES) by DSC. ê*J. Energy Storage* **2017**, *11*, 1–6. [CrossRef]
12. Cabeza, L.F.; Barreneche, C.; Martorell, I.; Miró, L.; Sari-Bey, S.; Fois, M.; Anghel, E.M. Unconventional experimental technologies available for phase change materials (PCM) characterization. Part 1. Thermophysical properties. *Renew. Sustain. Energy Rev.* **2015**, *43*, 1399–1414. [CrossRef]
13. Yinping, Z.; Yi, J. A simple method, the-history method, of determining the heat of fusion, specific heat and thermal conductivity of phase-change materials. *Meas. Sci. Technol.* **1999**, *10*, 201. [CrossRef]
14. Marín, J.M.; Zalba, B.; Cabeza, L.F.; Mehling, H. Determination of enthalpy–temperature curves of phase change materials with the temperature-history method: Improvement to temperature dependent properties. *Meas. Sci. Technol.* **2003**, *14*, 184. [CrossRef]
15. Hong, H.; Kim, S.K.; Kim, Y.S. Accuracy improvement of T-history method for measuring heat of fusion of various materials. *Int. J. Refrig.* **2004**, *27*, 360–366. [CrossRef]
16. Peck, J.H.; Kim, J.J.; Kang, C.; Hong, H. A study of accurate latent heat measurement for a PCM with a low melting temperature using T-history method. *Int. J. Refrig. 2006*, *29*, 1225–1232. [CrossRef]
17. Kravvaritis, E.D.; Antonopoulos, K.A.; Tzivanidis, C. Improvements to the measurement of the thermal properties of phase change materials. *Meas. Sci. Technol.* **2010**, *21*. [CrossRef]
18. Solé, A.; Miró, L.; Barreneche, C.; Martorell, I.; Cabeza, L.F. Review of the T-history method to determine thermophysical properties of phase change materials (PCM). *Renew. Sustain. Energy Rev.* **2013**, *26*, 425–436. [CrossRef]

19. Sandnes, B.; Rekstad, J. Supercooling salt hydrates: Stored enthalpy as a function of temperature. *Sol. Energy* **2006**, *80*, 616–625. [CrossRef]
20. Hasan, A.; McCormack, S.J.; Huang, M.J.; Norton, B. Characterization of phase change materials for thermal control of photovoltaics using Differential Scanning Calorimetry and Temperature History Method. *Energy Convers. Manag.* **2014**, *81*, 322–329. [CrossRef]
21. Kravvaritis, E.D.; Antonopoulos, K.A.; Tzivanidis, C. Experimental determination of the effective thermal capacity function and other thermal properties for various phase change materials using the thermal delay method. *Appl. Energy* **2011**, *88*, 4459–4469. [CrossRef]
22. Xu, T.; Gunasekara, S.N.; Chiu, J.N.; Palm, B.; Sawalha, S. Thermal behavior of a sodium acetate trihydrate-based PCM: T-history and full-scale tests. *Appl. Energy* **2020**, *261*. [CrossRef]
23. Babar, O.A.; Arora, V.K.; Nema, P.K. Selection of phase change material for solar thermal storage application: A comparative study. *J. Braz. Soc. Mech. Sci. Eng.* **2019**, *41*. [CrossRef]
24. Rady, M.A.; Arquis, E.; Le Bot, C. Characterization of granular phase changing composites for thermal energy storage using the T-history method. *Int. J. Energy Res.* **2010**, *34*, 333–344. [CrossRef]
25. Wang, X.; Dennis, M. Characterisation of thermal properties and charging performance of semi-clathrate hydrates for cold storage applications. *Appl. Energy* **2016**, *167*, 59–69. [CrossRef]
26. Yadav, C.; Sahoo, R.R. Experimental analysis for optimum thermal performance and thermophysical parameters of MWCNT based capric acid PCM by using T-history method. *Powder Technol.* **2020**, *364*, 392–403. [CrossRef]
27. Tan, P.; Brütting, M.; Vidi, S.; Ebert, H.P.; Johansson, P.; Kalagasidis, A.S. Characterizing phase change materials using the T-History method: On the factors influencing the accuracy and precision of the enthalpy-temperature curve. *Thermochim. Acta* **2018**, *666*, 212–228. [CrossRef]
28. Brütting, M.; Vidi, S.; Hemberger, F.; Ebert, H.P. Dynamic T-History method-A dynamic thermal resistance for the evaluation of the enthalpy-temperature curve of phase change materials. *Thermochim. Acta* **2019**, *671*, 161–169. [CrossRef]
29. Badenhorst, H.; Cabeza, L.F. Critical analysis of the T-history method: A fundamental approach. *Thermochim. Acta* **2017**, *650*, 95–105. [CrossRef]
30. Mazo, J.; Delgado, M.; Lázaro, A.; Dolado, P.; Peñalosa, C.; Marín, J.M.; Zalba, B. A theoretical study on the accuracy of the T-history method for enthalpy–temperature curve measurement: Analysis of the influence of thermal gradients inside T-history samples. *Meas. Sci. Technol.* **2015**, *26*. [CrossRef]
31. Moreno-Alvarez, L.; Herrera, J.N.; Meneses-Fabian, C. A differential formulation of the T-history calorimetric method. *Meas. Sci. Technol.* **2010**, *21*. [CrossRef]
32. Lazaro, A.; Günther, E.; Mehling, H.; Hiebler, S.; Marin, J.M.; Zalba, B. Verification of a T-history installation to measure enthalpy versus temperature curves of phase change materials. *Meas. Sci. Technol.* **2006**, *17*, 2168. [CrossRef]
33. Stanković, S.B.; Kyriacou, P.A. Improved measurement technique for the characterization of organic and inorganic phase change materials using the T-history method. *Appl. Energy* **2013**, *109*, 433–440. [CrossRef]
34. Yang, X.H.; Liu, J. A novel method for determining the melting point, fusion latent heat, specific heat capacity and thermal conductivity of phase change materials. *Int. J. Heat Mass Transf.* **2018**, *127*, 457–468. [CrossRef]
35. PCM RT-Line Wide-Ranging Organic PCM for Your Application. Available online: https://www.rubitherm.eu/en/index.php/productcategory/organische-pcm-rt (accessed on 1 June 2020).
36. Mehling, H.; Ebert, H.P.; Schossig, P. Development of standards for materials testing and quality control of PCM. In Proceedings of the 7th IIR Conference on Phase Change Materials and Slurries for Refrigeration and Air Conditioning, Dinan, France, 13–15 September 2006.
37. Colla, L.; Ercole, D.; Fedele, L.; Mancin, S.; Manca, O.; Bobbo, S. Nano-phase change materials for electronics cooling applications. *ASME J. Heat Transf.* **2017**, *139*. [CrossRef]